

# Formation Control of Underactuated Bio-inspired Snake Robots

Ehsan Rezapour · Kristin Y. Pettersen · Jan T. Gravdahl · Andreas Hofmann

Received: date / Accepted: date

**Abstract** This paper considers formation control of snake robots. In particular, based on a simplified locomotion model, and using the method of virtual holonomic constraints, we control the body shape of the robot to a desired gait pattern defined by some pre-specified constraint functions. These functions are dynamic in that they depend on the state variables of two compensators which are used to control the orientation and planar position of the robot, making this a dynamic maneuvering control strategy. Furthermore, using a formation control strategy we make the multi-agent system converge to and keep a desired geometric formation, and enforce the formation follow a desired straight line path with a given speed profile. Specifically, we use the proposed maneuvering controller to solve the formation control problem for a group of snake robots by synchronizing the commanded velocities of the robots. Simulation results are presented which illustrate the successful performance of the theoretical approach.

**Keywords** Formation control · Snake robots · Virtual holonomic constraints · Maneuvering control problem · Model-based control · Multi agent systems

---

E. Rezapour  
Norsk Titanium AS, Oslo, Norway  
Tel.: +47-40-573169  
E-mail: ehsan.rezapour@norsktitanium.no

K. Y. Pettersen, J. T. Gravdahl  
Department of Engineering Cybernetics, Norwegian University of Science and Technology (NTNU), Trondheim, Norway  
E-mail: {kristin.y.pettersen}{jan.tommy.gravdahl}@itk.ntnu.no

A. Hofmann  
Institute of Engineering and Computational Mechanics, University of Stuttgart, Stuttgart, Germany  
E-mail: andreas.hofmann@itm.uni-stuttgart.de

## 1 Introduction

Snake robots are a class of biologically-inspired robots which are inspired by structural characteristics of biological snakes. In contrast to the traditional locomotion tools, such as legs and wheels, snake robots offer interesting locomotion properties which make them capable of carrying out tasks in narrow and unstructured environments where wheels and legs might get tangled in the irregularities in the terrain. Furthermore, their hyper-redundant structure which is characterized by many degrees of freedom to perform a given task enables them to keep their mechanical stability even during the failure of some of their actuators.

The principal goal of this work is to design a model-based feedback control strategy for a group of snake robots such that each individual robot converges to and maintains its position in the formation, while the formation as a whole follows some pre-defined path with a desired velocity profile. To this end, we first design a dynamic feedback control law which controls the body shape of the robot to a desired gait pattern. Furthermore, we use the parameters of this gait pattern in the form of a static and a dynamic compensator which will be used in order to control the orientation and position of the robot in the plane. Moreover, by using a formation control strategy, we make the group of snake robots converge to and keep a desired formation, at the same time as the formation follows a desired straight line path with a given speed profile.

A variety of locomotion control problems for snake robots have been considered in previous works. The majority of these works consider snake robots with non-holonomic velocity constraints, which is inspired by the world's first snake robot developed in 1972 [1]. Non-holonomic constraints are in the form of sideslip con-

straints on the links of the robot, i.e. where each link is constrained from moving sideways. These nonholonomic constraints allow the control input to be defined directly in terms of the desired propulsion, which is employed in [2-4] for computed torque control of the position and orientation of snake robots. In [5], position and path following controllers are proposed for the case where some of the snake robot links are subject to sideslip constraints. These constrained links can be lifted from the ground, which provide the system with more degrees of freedom that can be utilized to follow a trajectory while simultaneously maintaining a high manipulability. In [6-7], based on a dynamic model, a control law for cooperative task of wheeled snake robots is derived. In [8], a Lyapunov-based path following control design for a snake robot subject to nonholonomic velocity constraints is proposed. Path following control of snake robots without nonholonomic velocity constraints is only considered in a few previous works. In [9], path following control of swimming snake robots is achieved by moving the joints according to a predetermined gait pattern while introducing an angular offset in each joint to control the orientation of the robot. Methods based on numerical optimal control are considered in [10] for determining optimal gaits during positional control of snake robots. In [11], a control strategy is proposed for sinus-lifting during lateral undulation by solving a quadratic optimization problem. In [12], the conditions for optimality of lateral undulatory locomotion of snake robots is studied using numerical simulations. In [13-14] cascaded systems theory is employed to achieve path following control of a snake robot described by a simplified locomotion model. In this simplified model of the snake robot, the motion of the links is approximated as translational displacements instead of rotational motion. This model is valid for small joint angles. In [15], a dynamic feedback controller are proposed which control the orientation of the robot to an angle defined by a path following guidance law and the theoretical approaches are validated through experimental results. In [16], using an input-output stability analysis, it is shown that the solutions of the dynamic compensator used in [15] for orientation control remain uniformly bounded. In [17], a direction following controller is proposed, which regulates the orientation and the forward velocity of the robot to constant references. A similar approach is used in [18-19], where the design is based on the simplified dynamic model for the snake robot which resolves the singularity in the control law derived in [17]. In [20], a maneuvering controller for the snake robot is derived using singular perturbation theory. In [21], controllability and stability analysis of planar snake robot locomotion is considered, and the sta-

bility results for a path following controller based on numerical investigations using Poincare maps are presented.

The main contribution of this paper is to design a model-based formation control strategy for a group of snake robots. Formation control is an attractive topic in control systems research, and many formation control strategies have been employed for various bio-inspired robotic systems and vehicles, see e.g. [22-25]. To our best knowledge, however, a similar formation control problem has never been considered for snake robots. Nonetheless, both in terms of theoretical developments and practical aspects, this is an important step forward for locomotion control of snake robots. In particular, the theoretical control challenges which arise due to the complicated dynamic model of snake robots, which have at least three degrees of underactuation, can contribute to an increased understanding of motion control of underactuated mechanical systems. Moreover, in terms of real-time applications, there are many advantages for mechanical systems which move in formation instead of using a single unit, since this can increase the robustness and efficiency of the operation, reduce costs, and also provide flexibility, agility, and more degrees of freedom for the system to perform more complex tasks, see [26-28]. These advantages can significantly empower the applications of snake robots in industrial operations.

The approach that we present here uses the theoretical results of [29] by application of reduction theorems for asymptotic stability of closed sets with application to backstepping control design. Path following and maneuvering control approaches for a single snake robot have previously been considered in e.g. [13], [20] and [39]. In particular, here we adapt the results and ideas of [20] which used a similar technique for addressing the maneuvering control problem to a different dynamic model of the snake robot. This resolves the singularity problem associated with the control law proposed in [20]. Moreover, as the main contribution of this paper we present a formation control strategy to make a group of snake robots follow a desired formation.

The paper is organized as follows. In Section 2, we present a simplified dynamic model of the snake robot that we will use for the model-based control design. In Section 3, we formulate our control design objectives. In Section 4, we design a dynamic feedback control law for the body shape of the robot. In Section 5, we present an orientation controller for the robot. In Section 6, we solve the maneuvering control problem for a single snake robot. In Section 7, we present our formation control strategy. Finally in Section 8, we present simulation results which show the performance of the proposed control strategies.

## 2 Modelling

In this section, we present the simplified dynamic model of a snake robot without nonholonomic velocity constraints which moves on a horizontal and flat surface. Here  $N$ ,  $l$ , and  $m$  denote the number, length and mass of the links, respectively. Based on the illustration of the robot in Fig. 1, we choose the generalized coordinates as  $x = [\phi_1, \dots, \phi_{N-1}, \theta, p_x, p_y]^T \in \mathbb{R}^{N+2}$ , where  $\phi_i$  denotes the  $i$ -th joint coordinate,  $\theta$  denotes the orientation, and  $(p_x, p_y)$  denotes the planar position of the center of mass (CM) of the robot. We denote the vector of the joint coordinates of the robot with  $\phi = [\phi_1, \dots, \phi_{N-1}]^T \in \mathbb{R}^{N-1}$ . The elements of  $\phi$  are called the body shape variables, which define the internal configuration of the robot. The vector of the generalized velocities is defined as the time-derivative of  $x$  as  $\dot{x} = [v_{\phi_1}, \dots, v_{\phi_{N-1}}, v_\theta, \dot{p}_x, \dot{p}_y]^T \in \mathbb{R}^{N+2}$ . We denote the vector of the joint velocities with  $v_\phi = [v_{\phi_1}, \dots, v_{\phi_{N-1}}]^T \in \mathbb{R}^{N-1}$ . The simplified model of the snake robot can be represented as [13]

$$\dot{\phi} = v_\phi \quad (1)$$

$$\dot{\theta} = v_\theta \quad (2)$$

$$\dot{p}_t = v_t \quad (3)$$

$$\dot{p}_x = v_t \cos(\theta) - v_n \sin(\theta) \quad (4)$$

$$\dot{p}_y = v_t \sin(\theta) + v_n \cos(\theta) \quad (5)$$

$$\dot{\phi} = \bar{u} \quad (6)$$

$$\dot{\theta} = -\lambda_1 v_\theta + \frac{\lambda_2}{N-1} v_t \bar{e}^T \phi \quad (7)$$

$$\dot{v}_t = -\frac{c_t}{m} v_t + \frac{2c_p}{Nm} v_n \bar{e}^T \phi - \frac{c_p}{Nm} \phi^T A \bar{D} v_\phi \quad (8)$$

$$\dot{v}_n = X v_\theta - Y \bar{v}_n \quad (9)$$

where  $\{v_t, v_n\} \in \mathbb{R}$  denote the tangential and normal components of the inertial velocity of the CM mapped into the direction of motion of the robot (see Fig. 1), respectively, and  $\{c_n, c_t\} \in \mathbb{R}_{>0}$  denote the viscous friction coefficients in the normal and tangential direction of motion of the links, respectively. Furthermore,  $\{\lambda_1, \lambda_2\} \in \mathbb{R}_{>0}$  are used to describe the mapping from the rotational motion to the prismatic motion (see [13]). These coefficients are chosen such that the simplified model quantitatively behaves similar to the more complex model of a snake robot which is described in [13]. Furthermore,  $c_p = \frac{c_n - c_t}{2l} > 0$ ,  $X = \epsilon \left( \frac{c_n}{m} - \lambda_1 \right)$ ,  $Y = \frac{c_n}{m}$ , and  $\epsilon = -\frac{2(N-1)c_p}{Nm\lambda_2}$ . Note that (6) represents the partially feedback linearized dynamics of the joint angles, where  $\bar{u} = [\bar{u}_1, \dots, \bar{u}_{N-1}]^T \in \mathbb{R}^{N-1}$  denotes the control input to the joints. Moreover,  $\bar{p}_y$  is the projection of  $p_y$  along the  $y$ -axis to a point where body shape changes of the robot generate a pure rotational motion and no sideways force. According to [13] this

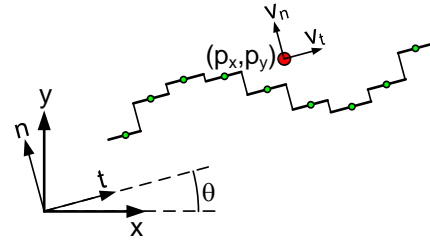


Fig. 1: Illustration of two coordinate frames used in the simplified model. The  $x - y$  frame is fixed, and the  $t - n$  frame is always aligned with the snake robot.

projection significantly simplifies the dynamics by removing the coupling between the dynamics of the joint and sideways motion. Finally,  $\bar{D}$ ,  $A$ , and  $\bar{e}$  are constant matrices and vectors which we refer to [13] for their definitions due to space restriction.

## 3 Control Design Objectives

In this section, the control design objectives for each snake robot will be defined. In order to solve the formation control problem, we need to solve the maneuvering control problem for each snake robot. Maneuvering control consists of two tasks [33]. The first task, called the geometric task, is to converge to and follow a desired geometric path. The second task, called the dynamic task, is to satisfy dynamical constraints, e.g. a desired velocity profile, along the desired path. In the following, we state the maneuvering control objectives for each snake robot, which stabilizes the motion of each robot w.r.t. a formation reference point (FRP).

- I. Given a desired gait pattern which produces forward locomotion  $\phi_{\text{ref}} : \mathbb{R} \rightarrow \mathbb{R}^{N-1}$ , we aim to asymptotically stabilize  $\phi - \phi_{\text{ref}} = 0$ .
- II. Given a desired orientation  $\theta_{\text{ref}}$  we aim to asymptotically stabilize  $\theta - \theta_{\text{ref}} = 0$ .
- III. Given a desired straight line path  $\xi = (p_{xd}, p_{yd}) \in \mathbb{R}^2$ , and assuming that the global  $x$ -axis is assigned such that it is always aligned with the desired straight path, i.e.  $p_{yd} \equiv 0$ , we aim to make the robot converge to the path such that the normal distance to the path, i.e. the cross-track error, converges to zero, i.e.  $\bar{p}_y \rightarrow 0$ .
- IV. Given a desired velocity along the path  $v_{t,\text{ref}}$  and a desired position  $p_{t,\text{ref}}(t) = \int_0^t v_{t,\text{ref}}(\tau) d\tau$  we aim to asymptotically stabilize  $p_t - p_{t,\text{ref}} = 0$  and  $v_t - v_{t,\text{ref}} = 0$ .

Furthermore, we require that all solutions of the controlled system remain uniformly bounded. Note that when Objective I is achieved the robot performs forward locomotion and  $\theta_{\text{ref}}$  will be designed such that

when Objective II is achieved the robot will be headed towards the path. Furthermore, when Objective III is achieved the normal distance of the robot to the path converges to zero, and Objective IV gives that the robot will move along the path, following a desired velocity profile, i.e. the tangential position and velocity errors will converge to zero.

The above control objectives will be achieved for each snake robot in the formation. Moreover, the ultimate goal for each robot is to maintain its position in the formation, i.e. w.r.t. the FRP, which will be achieved by synchronizing the desired velocity profiles of the robots, as we will see in Section 7.

#### 4 Body Shape Control

In this section, we propose a feedback control law for the body shape of the snake robot. In particular, we stabilize a desired gait pattern for the body shape variables, which induces lateral undulatory locomotion on the robot. Virtual holonomic constraints (VHC), see e.g. [30-32], are relations in configuration space  $\mathcal{Q}$  of the form  $\Phi : \mathcal{Q} \rightarrow \mathbb{R}$  which are called constraint functions, and they have the property that they can be made invariant by the actions of a feedback controller [31]. Inspired by the sinusoidal lateral undulatory gait introduced in [20], we define the following VHC, as the reference for the  $i$ -th joint angle of the robot:

$$\phi_{\text{ref},i}(\lambda, \phi_o) = \alpha \sin(\lambda + (i-1)\delta) + \phi_o \quad (10)$$

where  $\alpha$  denotes the amplitude of the joint oscillations, and  $\delta$  is a phase shift which is used to keep the joint out of phase. Moreover,  $\lambda \in \mathbb{S}$  and  $\phi_o \in \mathbb{R}$  are the solutions of two compensators which we will design to control the forward velocity and orientation of the robot, respectively. Note that  $\mathbb{S}$  denotes the one-dimensional sphere, i.e. the circle.

In particular, associated with the constraint functions (10), is the following *constraint manifold*

$$\Gamma_4 = \{(x, \dot{x}, \phi_o, \dot{\phi}_o, \lambda, \dot{\lambda}) \in \mathbb{R}^{2N+8} : \phi_i = \phi_{\text{ref},i}(\lambda, \phi_o), v_{\phi_i} = \dot{\lambda} \frac{\partial \phi_{\text{ref},i}}{\partial \lambda} + \dot{\phi}_o \frac{\partial \phi_{\text{ref},i}}{\partial \phi_o}\} \quad (11)$$

where  $i \in \{1, \dots, N-1\}$ . The blueprint of our control design approach is given in the following five steps:

1. In the first step, we use the control input  $\bar{u}$  in (6) to globally exponentially stabilize the constraint manifold (11) for the solutions of the dynamics of the body shape variables  $\phi$  of the robot. This induces a forward motion based on the gait pattern lateral undulation on the robot.
2. In the second step, we reduce the dynamics of the system to the globally invariant constraint manifold (11). On this manifold, we use  $\phi_o$  as an additional control term, which will be used to control the orientation of the robot.
3. In the third step, we use the frequency  $\dot{\lambda}$  of the periodic body motion, i.e. the gait pattern (10), as an additional control term to control the tangential position  $p_t$  and the tangential velocity  $v_t$  of the robot. This addresses the dynamic task of the maneuvering control.
4. In the fourth step, we find conditions for the controlled system such that the desired path is stabilized for the position  $\bar{p}_y$  and the normal velocity  $v_n$  of the robot. This addresses the geometric task of the maneuvering control.
5. In the fifth step, we define a FRP, and we stabilize the desired position of each snake robot w.r.t. this point, such that the group of snake robots moves in the desired geometric formation.

In order to enforce the VHC for the shape variables, i.e. to stabilize the constraint manifold for the shape variables  $\phi$ , we define the following input-output linearizing feedback control law:

$$\bar{u} = \ddot{\phi}_{\text{ref}} - K_d \dot{\tilde{\phi}} - K_p \tilde{\phi} \quad (12)$$

where  $\tilde{\phi} = [\phi_1 - \phi_{\text{ref},1}, \dots, \phi_{N-1} - \phi_{\text{ref},N-1}]^T \in \mathbb{R}^{N-1}$ ,  $K_p = \text{diag}\{k_{p_i}\}_{i=1}^{N-1}$  and  $K_d = \text{diag}\{k_{d_i}\}_{i=1}^{N-1}$  denote the positive definite diagonal gain matrices. By inserting (12) into (6), tracking error dynamics of the joint angles takes a globally exponentially stable form:

$$\ddot{\tilde{\phi}} + K_d \dot{\tilde{\phi}} + K_p \tilde{\phi} = 0. \quad (13)$$

Thus, control objective I will be achieved.

#### 5 Orientation Control

In this section, we control the orientation of the robot to a reference orientation angle defined by a path following guidance law. We will do this by choosing  $\phi_o$  as an additional control term through a static compensator on the exponentially stable constraint manifold.

We define the LOS path following guidance law, giving the reference orientation for the robot, as a function of the cross-track error as

$$\theta_{\text{ref}} = -\text{atan}\left(\frac{\bar{p}_y}{\Delta}\right) \quad (14)$$

where  $\Delta > 0$  is a design parameter that is called the look-ahead-distance. This parameter can be used to adjust the rate of convergence of the robot to the desired path, i.e. a smaller  $\Delta$  gives a faster convergence to the path. The idea of the LOS guidance law (14) is that steering the orientation of the snake robot such that

it is oriented towards a point located at a distance  $\Delta$  ahead of the robot on the desired path, will make the position of the robot converge to and follow the desired straight path.

To stabilize the reference orientation, we define the orientation error as  $\tilde{\theta} = \theta - \theta_{\text{ref}}$ . The orientation error dynamics evaluated on the constraint manifold is

$$\ddot{\tilde{\theta}} = -\lambda_1 \dot{\tilde{\theta}} - \lambda_1 \dot{\theta}_{\text{ref}} + \frac{\lambda_2}{N-1} v_t \bar{e}^T S + \lambda_2 v_t \phi_o - \ddot{\theta}_{\text{ref}} \quad (15)$$

where  $S = [\alpha \sin(\lambda), \dots, \alpha \sin(\lambda + (i-1)\delta)]^T \in \mathbb{R}^{N-1}$ . We define the following *orientation control manifold*, which we aim to exponentially stabilize relative to  $\Gamma_4$ :

$$\Gamma_3 = \{(\theta, \dot{\theta}, \phi_o, \dot{\phi}_o, v_t, \lambda) \in \Gamma_4 : (\tilde{\theta}, \dot{\tilde{\theta}}) = (0, 0), \|[\phi_o, \dot{\phi}_o]\| \leq \epsilon_\phi\} \quad (16)$$

where  $\epsilon_\phi > 0$  is a positive constant. Note that stabilizing  $\Gamma_3$  relative to  $\Gamma_4$  implies that the orientation error converges exponentially to zero on the constraint manifold, and control objective II will be achieved. Furthermore, we will show how this implies the boundedness of the solutions of the static compensator which controls the orientation of the robot.

In order to stabilize the origin  $(\tilde{\theta}, \dot{\tilde{\theta}}) = (0, 0)$  of (15), we define the additional control input  $\phi_o$  as

$$\phi_o = \frac{1}{\lambda_2 v_t} \left( -\frac{\lambda_2}{N-1} v_t \bar{e}^T S + \lambda_1 \dot{\theta}_{\text{ref}} + \ddot{\theta}_{\text{ref}} - k_\theta \tilde{\theta} \right) \quad (17)$$

where  $k_\theta > 0$  denotes the proportional orientation controller gain. Note that on the constraint manifold, where a lateral undulatory gait is stabilized, the tangential velocity  $v_t$  is bounded away from zero and thus (17) is well-defined. By inserting (17) into (15), the orientation error dynamics of the robot evaluated on the constraint manifold takes a globally exponentially stable form:

$$\ddot{\tilde{\theta}} + \lambda_1 \dot{\tilde{\theta}} + k_\theta \tilde{\theta} = 0. \quad (18)$$

Thus, control objective II will be achieved.

**Remark 1.** *Provided that  $v_t$  has no finite-escape time (see Proposition 2), it can be shown that the static compensator (17) will be uniformly ultimately bounded by  $\|\phi_o\| \leq \alpha$  where  $\alpha$  denotes the amplitude of the reference joint angles (10).*

**Remark 2.** *Inserting (10) into (12), it can be seen that the second order time-derivative of the control input  $\phi_o$  is needed for the joint control law (12). However,  $\dot{\phi}_o$  and  $\ddot{\phi}_o$  are complicated functions of time that cannot be easily computed analytically. In order to compute these terms, we take the approach given in [34], by using a second order low-pass filtering reference model. In particular, we compute these time-derivatives by passing  $\phi_o$  through a low-pass filter of the form*

$$\dot{\Omega} = \begin{bmatrix} 0 & 1 \\ -\omega_n^2 & -2\psi_f \omega_n \end{bmatrix} \Omega + \begin{bmatrix} 0 \\ \omega_n^2 \end{bmatrix} \phi_o \quad (19)$$

with natural frequency  $\omega_n$  and damping ratio  $\psi_f$ . This filter is an input-to-state stable system, see e.g. [36]. This implies that the output  $\dot{\phi}_o$  remains bounded. Consequently, for the two other dynamical subsystems which govern the dynamics of the position of the CM of the robot, we take  $\dot{\phi}_o$  as a bounded exogenous signal which will be cancelled through the action of a dynamic compensator given by (35) which will be designed to control the position of the robot in the next section.

**Proposition 1.** *The control law governed by the solution of the static compensator (17), asymptotically stabilizes  $\Gamma_3$  relative to  $\Gamma_4$ . Furthermore, provided that  $v_t$  has no finite-escape time, see Proposition 3, the solutions of the static compensator (17) remain uniformly ultimately bounded by the ultimate bound  $\epsilon_\phi = \alpha$ .*

## 6 Maneuvering Control

In this section, we address the maneuvering problem by utilizing the idea of velocity control for snake robots given in [20]. To this end, we derive a dynamic compensator which controls the velocity and position of the robot along the desired path by using the frequency of the joint oscillations as an additional control term. In particular, we define a *velocity control manifold* which we aim to exponentially stabilize relative to the constraint manifold  $\Gamma_4$  for the closed-loop system as

$$\Gamma_2 = \{(\theta, \dot{\theta}, p_t, v_t, v_n, \phi_o, \dot{\phi}_o, \lambda, \dot{\lambda}) \in \Gamma_4 : (\tilde{\theta}, \dot{\tilde{\theta}}) = (0, 0), (\tilde{p}_t, \tilde{v}_t) = (0, 0), \|v_n\| \leq \epsilon_n, \|[\phi_o, \dot{\phi}_o]\| \leq \epsilon_\phi, \|[\lambda, \dot{\lambda}]\| \leq \epsilon_\lambda\} \quad (20)$$

where  $\epsilon_n > 0$ ,  $\epsilon_\phi > 0$ , and  $\epsilon_\lambda > 0$  are constants. Thus, stabilizing  $\Gamma_2$  relative to the constraint manifold  $\Gamma_4$  implies that the robot will follow the reference orientation defined by (14), and a reference velocity which will be defined below. Furthermore, the static compensator (17) which controls the orientation of the robot remains bounded. Moreover, the solutions of the dynamic compensator which will be designed in this section to control the forward velocity of the robot will remain bounded. We start by showing the boundedness of  $v_n$ . In particular, since the normal velocity  $v_n$  is coupled with the dynamics of the tangential velocity  $v_t$ , then we need to investigate the boundedness of this variable, in order to ensure that while we control the tangential velocity to a reference signal, the normal velocity remains stable, i.e. we need to analyze the stability of internal dynamics.

**Theorem 1.** *Under the joint controller (12) and the orientation controller (17), the normal velocity  $v_n$  of the robot is uniformly bounded.*

*Proof:* we start by selecting a Lyapunov function candidate  $V = \frac{1}{2}\bar{v}_n^2$ . Taking the time-derivative of  $V$  along (9) we get  $\dot{V} = X\bar{v}_n v_\theta - Y\bar{v}_n^2$ . Using Young's inequality we get  $\dot{V} \leq (-Y + \gamma|X|/2)\bar{v}_n^2 + |X|v_\theta^2/2\gamma$ , where  $\gamma$  is any positive constant. From the stability result of the previous section, and assuming that  $v_t$  has no finite escape time (see Proposition 2) we conclude that  $|X|v_\theta^2/2\gamma \leq \beta_1$  where  $\beta_1$  is a positive constant. Furthermore, by choosing a sufficiently small  $\gamma$  we can show that  $\dot{V} \leq -\beta_2 V + \beta_1$ , where  $\beta_2$  is a sufficiently small positive constant. Now, by Comparison Lemma [35] it is straightforward to show that  $\|v_n\| \leq \epsilon_n$ , for some  $\epsilon_n > 0$ . This bound is governed by the friction coefficient  $c_n$ .

### 6.1 Maneuvering Control: The Dynamic Task

In this subsection, we address the dynamic task by controlling the position and velocity of the robot along the desired path. In particular, motivated by [20], we use the frequency of the joint angle oscillations as an additional control term in order to control the forward velocity of the robot to a reference velocity. To this end, we define the tangential position error  $\tilde{p}_t = p_t - p_{t,\text{ref}}$  and velocity error  $\tilde{v}_t = v_t - v_{t,\text{ref}}$ . Furthermore, we derive the position and velocity error dynamics evaluated on the constraint manifold (11) as

$$\begin{aligned} \dot{\tilde{p}}_t &= \tilde{v}_t \\ \dot{\tilde{v}}_t &= -\frac{c_t}{m}(\tilde{v}_t + v_{t,\text{ref}}) + \frac{2c_p}{Nm}v_n \bar{e}^T \Phi_{\text{ref}} + \eta \left( \dot{\lambda} C + \dot{\phi}_o \bar{e} \right) \\ &\quad - \dot{v}_{t,\text{ref}} \end{aligned} \quad (21)$$

where  $C$ ,  $\Phi_{\text{ref}}$  and  $\eta$  are defined as:

$$\begin{aligned} C &= [\alpha \cos(\lambda), \dots, \alpha \cos(\lambda + (i-1)\delta)]^T \in \mathbb{R}^{N-1} \\ \Phi_{\text{ref}} &= [\phi_{\text{ref},1}, \dots, \phi_{\text{ref},N-1}]^T \in \mathbb{R}^{N-1} \\ \eta &= -\frac{c_p}{Nm} \Phi_{\text{ref}}^T A \bar{D} \in \mathbb{R}^{N-1}. \end{aligned}$$

In the following, we use  $u_\lambda = \dot{\lambda}$  as the control input to stabilize the origin  $(\tilde{p}_t, \tilde{v}_t) = (0, 0)$  of (21). In particular, we iteratively introduce Control-Lyapunov functions (CLF) borrowing the techniques of backstepping (see e.g. [36]). We select the first CLF of the form

$$V_1 = \frac{1}{2}\tilde{p}_t^2. \quad (22)$$

Taking the time-derivative of (22) along the solutions of (21) yields  $\dot{V}_1 = \tilde{p}_t \dot{\tilde{p}}_t = \tilde{p}_t (v_t - v_{t,\text{ref}})$ . We take  $v_t$  as a virtual control input which we utilize to make  $\dot{V}_1$  negative. In particular, we define

$$v_t = v_{t,\text{ref}} - k_{z_0} \tilde{p}_t \quad (23)$$

where  $k_{z_0} > 0$  is a constant gain. We define the error variable

$$z_1 = v_t - v_{t,\text{ref}} + k_{z_0} \tilde{p}_t \quad (24)$$

that we aim to drive to zero. Thus, we can rewrite:

$$\dot{V}_1 = -k_{z_0} \tilde{p}_t^2 + z_1 \tilde{p}_t. \quad (25)$$

To perform backstepping for  $z_1$ , we write the error dynamics for the error variable which has the form

$$\dot{z}_1 = \dot{v}_t - \dot{v}_{t,\text{ref}} + k_{z_0} \dot{\tilde{p}}_t = \dot{\tilde{v}}_t + k_{z_0} \dot{\tilde{p}}_t \quad (26)$$

We choose an augmented CLF of the form

$$V_2 = V_1 + \frac{1}{2}z_1^2. \quad (27)$$

Taking the time-derivative of  $V_2$  along the solutions of (21) yields

$$\begin{aligned} \dot{V}_2 &= -k_{z_0} \tilde{p}_t^2 + z_1 (\tilde{p}_t + \dot{\tilde{v}}_t + k_{z_0} \dot{\tilde{p}}_t) \\ &= -k_{z_0} \tilde{p}_t^2 + z_1 \left( \tilde{p}_t - \frac{c_t}{m} z_1 - \frac{c_t}{m} v_{t,\text{ref}} + \frac{c_t}{m} k_{z_0} \tilde{p}_t \right. \\ &\quad \left. + \frac{2c_p}{Nm} v_n \bar{e} \Phi_{\text{ref}} + \eta C \dot{\lambda} + \eta \bar{e} \dot{\phi}_o - \dot{v}_{t,\text{ref}} + k_{z_0} \dot{\tilde{p}}_t \right). \end{aligned} \quad (28)$$

We denote  $\delta_1(\phi_o, \lambda) = \eta C$ . Due to the phase shift between the link references in (10), it can be numerically verified that  $\delta_1(\cdot)$  is uniformly bounded away from zero. We take  $\dot{\lambda}$  as a virtual control input that we use to make (28) negative:

$$\begin{aligned} \dot{\lambda} &= \frac{1}{\delta_1} \left( -\tilde{p}_t + \frac{c_t}{m} v_{t,\text{ref}} - \frac{c_t}{m} k_{z_0} \tilde{p}_t - \frac{2c_p}{Nm} v_n \bar{e} \Phi_{\text{ref}} \right. \\ &\quad \left. - \eta \bar{e} \dot{\phi}_o + \dot{v}_{t,\text{ref}} - k_{z_0} \dot{\tilde{p}}_t - k_{z_1} z_1 \right) \end{aligned} \quad (29)$$

where  $k_{z_1} > 0$  is a constant gain. For simplicity, we denote

$$\begin{aligned} \delta_2(\phi_o, \dot{\phi}_o, \lambda, p_t, v_t) &= \\ &= \frac{1}{\delta_1} \left( -\tilde{p}_t + \frac{c_t}{m} v_{t,\text{ref}} - \frac{c_t}{m} k_{z_0} \tilde{p}_t - \frac{2c_p}{Nm} v_n \bar{e} \Phi_{\text{ref}} \right. \\ &\quad \left. - \eta \bar{e} \dot{\phi}_o + \dot{v}_{t,\text{ref}} - k_{z_0} \dot{\tilde{p}}_t - k_{z_1} z_1 \right). \end{aligned} \quad (30)$$

Note that we could have chosen  $\dot{\lambda}$  to be given by the compensator in (29). However, since (29) represents the frequency of the lateral undulation motion given in (10) it is desirable from a practical implementation point of view to smooth the frequency function. We thus introduce an extra step of backstepping, and define the second error variable as  $z_2 = \dot{\lambda} - \delta_2$  which we aim to drive to zero. Inserting  $\dot{\lambda} = z_2 + \delta_2$  into (28) yields

$$\dot{V}_2 = -k_{z_0} \tilde{p}_t^2 - \left( \frac{c_t}{m} + k_{z_1} \right) z_1^2 + z_1 z_2 \delta_1. \quad (31)$$

To perform backstepping for  $z_2$ , we write the error dynamics for the error variable  $z_2$  which has the form

$$\dot{z}_2 = u_\lambda - \dot{\delta}_2. \quad (32)$$

We choose the augmented CLF in the form

$$V_3 = V_2 + \frac{1}{2}z_2^2. \quad (33)$$

The time-derivative of  $V_3$  along the solutions of (21) is

$$\dot{V}_3 = -k_{z_0}\tilde{p}_t^2 - \left(\frac{c_t}{m} + k_{z_1}\right)z_1^2 + z_2\left(z_1\delta_1 + u_\lambda - \dot{\delta}_2\right). \quad (34)$$

We define the velocity control input  $u_\lambda$  in the form

$$u_\lambda = -z_1\delta_1 + \dot{\delta}_2 - k_{z_2}z_2 \quad (35)$$

where  $k_{z_2} > 0$  is a constant gain. Inserting (35) into (34) yields

$$\dot{V}_3 = -k_{z_0}\tilde{p}_t^2 - \left(\frac{c_t}{m} + k_{z_1}\right)z_1^2 - k_{z_2}z_2^2. \quad (36)$$

From (36), it can be shown that  $\dot{V}_3 \leq -\beta_3 V_3$  where  $\beta_3 \in \mathbb{R}_{>0}$  is a sufficiently small positive constant. This implies that the origin  $(\tilde{p}_t, \tilde{v}_t) = (0, 0)$  of (21) is exponentially stable and the control objective IV will be achieved. Furthermore, since  $\dot{\lambda} = z_2 + \delta_2$  where  $z_2$  converges to zero and  $\delta_2$  is uniformly bounded, then  $\dot{\lambda}$  remains uniformly bounded. We denote the bound on the solutions of the dynamic compensator (35) with  $\|[\lambda, \dot{\lambda}]\| \leq \epsilon_\lambda$ .

**Proposition 2.** *Under the the controllers (12), (17), and (35), with the augmented state vector*

$$x = [p_t, v_t, p_n, v_n, \phi_o, \dot{\phi}_o, \lambda, \dot{\lambda}] \in \mathbb{R}^8$$

*the closed-loop tangential and normal position dynamics along with the dynamics of the compensators take the form  $\dot{x} = f(x)$ . Since throughout our stability proof we showed that all the functions in the closed-loop remain bounded, then it can be shown that  $\|f(x)\| \leq K(1 + \|x\|)$  where  $K \in \mathbb{R}_{>0}$  is a constant. This linear growth condition implies that none of the components of the state vector  $x$  have finite escape time, which validates the results presented in this section which were derived based on this assumption.*

**Proposition 3.** *Using the controllers (12), (17) and (35), the velocity control manifold  $\Gamma_2$  is asymptotically stable relative to the constraint manifold  $\Gamma_4$ .*

## 6.2 Maneuvering Control: The Geometric Task

So far we have controlled the body shape, orientation, and the position of the robot along the tangential axis of the  $t - n$  frame. The last step of our maneuvering control design is to stabilize the normal position  $\bar{p}_y$  of the robot to the desired path. Note that this will imply the convergence of the cross-track error to zero. Also note that we have already proved the boundedness of the normal velocity  $\bar{v}_n$  of the robot in the previous section.

Also we define the *path following manifold*, i.e. the manifold on which the geometric task is achieved, as

$$\Gamma_1 = \left\{ (\theta, \dot{\theta}, p_t, v_t, \bar{p}_y, v_n, \phi_o, \dot{\phi}_o, \lambda, \dot{\lambda}) \in \Gamma_2 : \bar{p}_y \leq \epsilon_p \right\}$$

(37)

where  $\epsilon_p \in \mathbb{R}_{>0}$  is any constant. In order to make  $\bar{p}_y \rightarrow 0$ , and thereby achieve control objective III we consider the dynamics of the position of the CM given by

$$\dot{\bar{p}}_y = v_t \sin(\theta) + v_n \cos(\theta) \quad (38)$$

which in the error coordinates can be written as

$$\dot{\bar{p}}_y = (\tilde{v}_t + v_{t,\text{ref}}) \sin(\tilde{\theta} + \theta_{\text{ref}}) + \tilde{v}_n \cos(\tilde{\theta} + \theta_{\text{ref}}) \quad (39)$$

The reduced dynamics of the position of the CM evaluated on the exponentially stable manifold  $\Gamma_2$ , is of the form

$$\dot{\bar{p}}_y = v_{t,\text{ref}} \sin(\theta_{\text{ref}}) + \tilde{v}_n \cos(\theta_{\text{ref}}). \quad (40)$$

By using the relations

$$\sin\left(-\text{atan}\left(\frac{\bar{p}_y}{\Delta}\right)\right) = -\frac{\bar{p}_y}{\sqrt{\bar{p}_y^2 + \Delta^2}}, \quad (41)$$

$$\cos\left(-\text{atan}\left(\frac{\bar{p}_y}{\Delta}\right)\right) = \frac{\Delta}{\sqrt{\bar{p}_y^2 + \Delta^2}} \quad (42)$$

we can rewrite (40) as

$$\dot{\bar{p}}_y = -\frac{v_{t,\text{ref}}\bar{p}_y}{\sqrt{\bar{p}_y^2 + \Delta^2}} + \frac{\tilde{v}_n\Delta}{\sqrt{\bar{p}_y^2 + \Delta^2}}. \quad (43)$$

We select a Lyapunov function candidate of the form

$$V = \frac{1}{2}\bar{p}_y^2. \quad (44)$$

Taking the time-derivative of (44) along the solutions of (43), and utilizing the stability results above, yields

$$\begin{aligned} \dot{V} &= \bar{p}_y \left( -\frac{v_{t,\text{ref}}\bar{p}_y}{\sqrt{\bar{p}_y^2 + \Delta^2}} + \frac{\tilde{v}_n\Delta}{\sqrt{\bar{p}_y^2 + \Delta^2}} \right) \\ &\leq -\left( \frac{v_{t,\text{ref}}}{\sqrt{\bar{p}_y^2 + \Delta^2}} \right) \bar{p}_y^2 + \epsilon_n \|\bar{p}_y\| \\ &\leq -\left( \frac{v_{\min}}{\sqrt{\bar{p}_y^2 + \Delta^2}} \right) \bar{p}_y^2 + \epsilon_n \left( \frac{\gamma\bar{p}_y^2}{2} + \frac{1}{2\gamma} \right) \end{aligned} \quad (45)$$

where we used Young's inequality, and where  $v_{\min}$  denotes the minimum forward velocity of the robot. Note that according to the results of [20], a snake robot with zero forward velocity is not controllable. Finally, we have

$$\dot{V} \leq \left( -\frac{v_{\min}}{\sqrt{\bar{p}_y^2 + \Delta^2}} + \frac{\epsilon_n\gamma}{2} \right) \bar{p}_y^2 + \eta \quad (46)$$

where  $\eta = \epsilon_n/2\gamma$ . We investigate two possible scenarios for the time-derivative of  $V$  in (46).

1. In the first scenario, it can be seen that for given parameters  $(v_{\min}, \Delta, \epsilon_n)$ , we can always choose a sufficiently small  $\gamma$  such that the coefficient of  $\bar{p}_y^2$  in (46) is negative. In this case, we conclude that there exist

a sufficiently small positive constant  $\beta \in \mathbb{R}_{>0}$ , such that  $\dot{V} \leq -\beta V + \eta$ . Using the Comparison Lemma, we have

$$V(t) \leq V(0)e^{-\beta t} + \frac{\eta}{\beta}. \quad (47)$$

This implies that  $V$  converges to a ball of radius  $\frac{\eta}{\beta}$ . Furthermore, because of (44), we can conclude that  $\bar{p}_y$  converges to a ball of the radius  $\sqrt{\frac{2\eta}{\beta}}$ , i.e. the equilibrium  $\bar{p}_y = 0$  of (43) is stable.

- In the second scenario, we would like to drive the cross-track error  $\bar{p}_y$ , to an arbitrary small neighbourhood of zero which we denote by  $\epsilon_p \in \mathbb{R}_{>0}$  for any positive constant  $\epsilon_p$ , i.e. we seek practical stability for the origin of (43). In this case, we choose

$$\gamma = \frac{\epsilon_n \beta}{2 \epsilon_p^2}. \quad (48)$$

Substituting (48) into (47) yields

$$V(t) \leq V(0)e^{-\beta t} + \epsilon_p^2 \quad (49)$$

which implies that  $\bar{p}_y$  converges to a ball of the radius  $\epsilon_p$ . In this case we must have the following conditions on the parameters  $(v_{\min}, \epsilon_n)$  such that the coefficient of  $\bar{p}_y^2$  is negative.

- The minimum tangential velocity  $v_{\min}$  should be sufficiently large.
- The upper-bound on the normal velocity of the robot  $v_n$  should be sufficiently small. From Theorem 1, this implies that the friction coefficient in the normal direction of motion  $c_n$  must be sufficiently large.

The above conditions guarantee that the path following error  $\bar{p}_y$  converges to an arbitrarily small neighbourhood of the origin, which readily implies that we will solve the geometric task. Fig. 2 shows the structure of the proposed maneuvering controller. Finally, we collect all the established stability results in the following theorem, which states that the proposed maneuvering controller solves the dynamic and geometric tasks.

**Remark 3.** *The path following set  $\Gamma_1$  is a compact set. This is due to the fact that all the variables  $(\theta, \dot{\theta}, p_t, v_t, \bar{p}_y, v_n, \phi_o, \dot{\phi}_o, \lambda, \dot{\lambda})$  used to define this set were proved to be bounded, which implies the compactness, i.e. boundedness, of the set.*

**Theorem 2.** *Consider the positively invariant sets  $\Gamma_4, \Gamma_3$ , and  $\Gamma_2$  and  $\Gamma_1$  in (11), (16), (20), and (37), respectively. Note that  $\Gamma_1 \subset \Gamma_2 \subset \Gamma_3 \subset \Gamma_4 \subset \mathcal{Q}$ , where  $\mathcal{Q}$  denotes the configuration space. The set  $\Gamma_1$  is a compact set. For  $i = 1 \dots 3$ , the set  $\Gamma_i$  was asymptotically stable relative to  $\Gamma_{i+1}$ . Consequently, according to Proposition 14 in [29], the set  $\Gamma_1$  is asymptotically stable for the controlled system. This implies that all the control objectives I-IV will be achieved, and all the solutions of the controlled system remain uniformly bounded.*

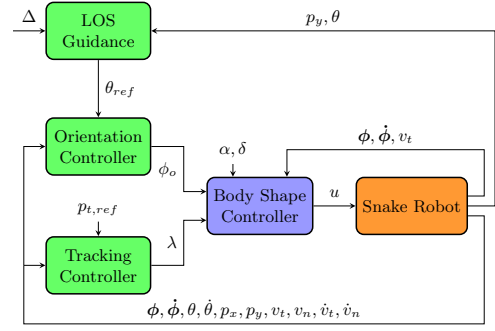


Fig. 2: The structure of the maneuvering controller

## 7 Formation Control

In this section, we address the cross-track formation control of a group of snake robots. To this end, for each snake robot we use the proposed cross-track controller for which we showed that the control objectives I-IV will be achieved. Furthermore, following the formation control strategy in [38] we use the desired velocity of each robot as the control term for synchronizing the motion of the robots along the desired paths. Since in this section we are dealing with multiple snake robots, we will use the superscript  $j \in \{1, \dots, n\}$  to denote the robot's number.

Under the controller (35), the velocity dynamics of the  $j$ -th robot in closed-loop is given as

$$\dot{v}_t^j = v_{t,\text{ref}}^j - k_{z0} \tilde{p}_t^j \quad (50)$$

We showed that the cross-track control goal is achieved provided that the desired speed for each snake lies inside the set  $(v_{\min}, v_{\max})$ . Thus, here we assume that the desired speed profile is within  $(v_{\min}, v_{\max})$ , i.e. there exists  $a > 0$  s.t.  $v_{t,\text{ref}} \in [v_{\min} + a, v_{\max} - a]$ ,  $t \geq 0$ . To solve the formation control problem, each snake should adjust its speed to asymptotically converge to the desired geometric formation and move according to the desired velocity profile  $v_d \in \mathbb{R}_{>0}$ . Thus, by adapting the results of [37-38] to our proposed maneuvering controller, we define the following formation control law defined through the reference velocity of each snake  $v_{t,\text{ref}}^j$ :

$$v_{t,\text{ref}}^j = v_d + g \left( \sum_{i=1}^n \gamma_{ji} (p_x^j - p_x^i) - d_{ji} \right) \quad (51)$$

where  $j = 1, \dots, n$ . Here  $d_{ji} = D_{x_j} - D_{x_i}$  correspond to the desired distances along the  $x$ -axis between the  $j$ -th and  $i$ -th snakes in the formation. The linkage parameters  $\gamma_{ji}$  are nonnegative and satisfy  $\gamma_{ij} = \gamma_{ji}$ ,  $\gamma_{ii} = 0$ . The function  $g(x)$  is a continuously differentiable non-decreasing function with a bounded derivative satisfying  $g'(0) > 0$ ,  $g(0) = 0$  and  $g(x) \in (-a, a)$ , where  $a$  was the parameter defined above. Following [36-37], the function  $g$  can be chosen, for example, equal to  $g(x) = (2a/\pi) \text{atan}(x)$ . Inserting (51) into (50), the ve-

locity dynamics of the robot takes the form

$$v_t^j = v_d + g \left( \sum_{i=1}^n \gamma_{ji} (p_x^j - p_x^i) - d_{ji} \right) - k_{z_0} \tilde{p}_t^j \quad (52)$$

Using the change of coordinates  $\hat{p}_x^j = p_x^j - D_{x_j} - \int_0^t v_d(s) ds$ , we can rewrite:

$$\dot{\hat{p}}_x^j = -g \left( \sum_{i=1}^n \gamma_{ji} (\hat{p}_x^j - \hat{p}_x^i) \right) - k_{z_0} \tilde{p}_t^j. \quad (53)$$

Using the notations  $\hat{p}_x = [\hat{p}_x^1, \dots, \hat{p}_x^n]^T$ ,  $g(\hat{p}_x) = [g(\hat{p}_x^1), \dots, g(\hat{p}_x^n)]^T$ , and  $\tilde{p}_t = [\tilde{p}_t^1, \dots, \tilde{p}_t^n]^T$  we have

$$\dot{\hat{p}}_x = -g(\Gamma \hat{p}_x) - k_{z_0} \tilde{p}_t \quad (54)$$

where the matrix  $\Gamma$  is given by

$$\Gamma = \begin{bmatrix} \sum_{j=1}^n \gamma_{1j} & -\gamma_{12} & \dots & -\gamma_{1n} \\ -\gamma_{21} & \sum_{j=1}^n \gamma_{2j} & \dots & -\gamma_{2n} \\ \vdots & \vdots & \ddots & \vdots \\ -\gamma_{n1} & -\gamma_{n2} & \dots & \sum_{j=1}^n \gamma_{nj} \end{bmatrix}. \quad (55)$$

The matrix  $\Gamma$  has the property  $\Gamma v_1 = 0$ , where  $v_1 = [1, 1, \dots, 1]^T$ . This implies that  $\Gamma$  has one zero eigenvalue, for which  $v_1$  denotes the corresponding eigenvector [38]. For some constant  $c \in \mathbb{R}$ , the formation control objective for the system (54) can be given as

$$\hat{p}_x(t) \rightarrow c v_1, \quad t \rightarrow +\infty \quad (56)$$

Using the results of [37-38], we present the following theorem which considers the achievement of the desired formation.

**Theorem 3.** Consider system (54) coupled with the error dynamics of every snake robot through  $k_{z_0} \tilde{p}$ . Suppose that the conditions of Theorem 2 hold for every snake robot and that the zero eigenvalue of matrix  $\Gamma$  has multiplicity one. Then the control goal (56) is achieved exponentially.

The proof is based on cascaded systems theory and follows along the same lines as for [38, Theorem 2].

## 8 Simulation Results

To illustrate the performance of the proposed formation controller, we present simulation results for three snake robots which should move in a given triangular formation. In particular, we aim to make three robots achieve a triangular formation where both the normal and tangential distances between the robot ( $j = 2$ ) - which is initially located on  $(p_x^2, p_y^2) = (0, 0)$  - and two robots ( $j = 1, 3$ ) is 1 m, i.e. we require  $d_{12} = -1$ ,  $d_{13} = 0$ ,  $d_{23} = 1$ . The simulation parameters were  $N = 10$ ,  $l = 0.14$  m,  $m = 1$  kg, and friction coefficients  $c_t = 1$  and  $c_n = 3$ ,  $\lambda_1 = 0.5$  and  $\lambda_2 = 20$ . The gait parameters were  $\alpha = 0.045$  m and  $\delta = 40\pi/180$ . The controller

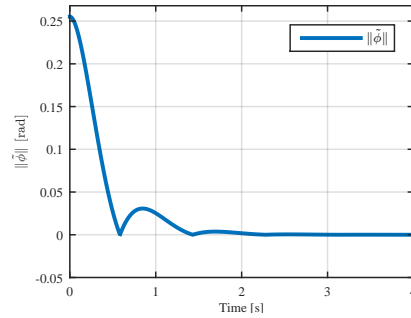


Fig. 3: Exponential stability of the joints tracking errors.

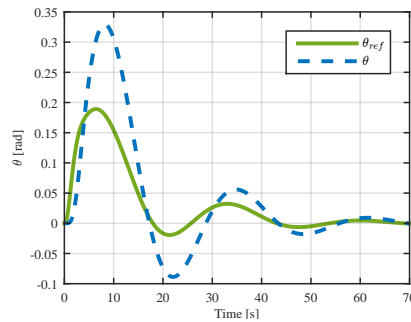


Fig. 4: Orientation reference tracking and orientation error.

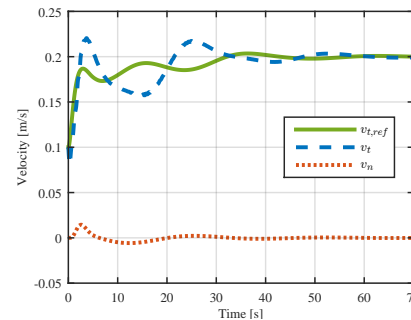


Fig. 5: Forward and sideways velocities with references.

gains were  $k_p = 20$ ,  $k_d = 5$ ,  $k_\theta = 0.1$ ,  $k_{z_0} = 5$ ,  $k_{z_1} = 0.5$  and  $k_{z_2} = 0.1$ . The tangential velocity of the FRP along the path was  $v_d = 0.2$  m/s, and the position reference was  $p_{t,\text{ref}} = \int v_{t,\text{ref}} dt$ . The look ahead distance was  $\Delta = 2.8$  m. To avoid singularities the initial tangential velocity was set to  $v_t(0) = 0.1$  m/s, see the arguments after (17). All the other states were set initially to zero. The simulation results are presented in Fig. 3-7 for one snake robot as an example. In particular, these figures show that the robot successfully achieves control Objectives I-IV. Furthermore, Fig. 8-11 present the results of the formation control, and show that the group achieves the desired triangular formation by synchronizing the reference velocity of each snake robot.

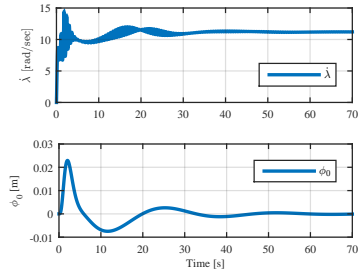


Fig. 6: The joint oscillation frequency  $\dot{\lambda}$  converges to a positive constant and the joint offset  $\phi_0$  is bounded and becomes zero.

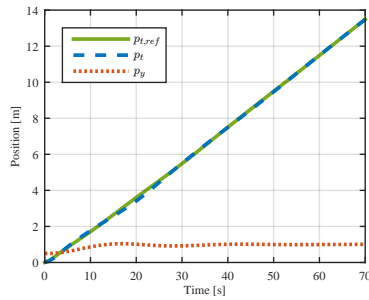


Fig. 7: Snake robot  $j = 1$  converges to  $p_y^1 = 1$  and follows the reference position.

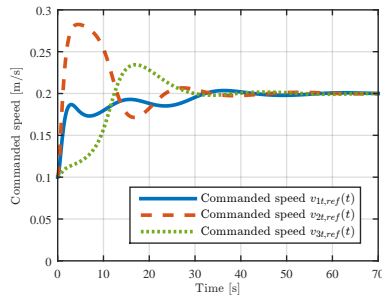


Fig. 8: The reference velocities converge to the desired speed profile of the formation  $v_d = 0.2$  m/s after compensating the formation error

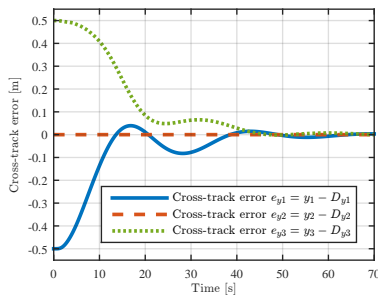


Fig. 9: The cross-track errors of all snake robots converge to zero

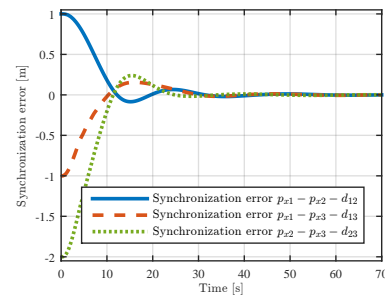


Fig. 10: The synchronization errors defined in (51) converge to zero

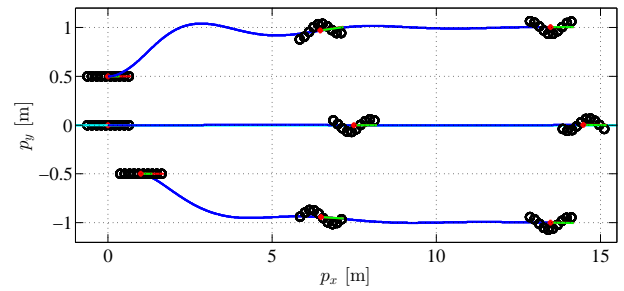


Fig. 11: Snake robots move in the desired geometric formation

## 9 Conclusion and Future Work

This paper considered maneuvering formation control of planar snake robots, using the method of virtual holonomic constraints. We first proposed a maneuvering controller for a planar snake robot, which was derived based on the simplified model of snake robot locomotion presented in [13]. The maneuvering controller was hierarchically designed in two steps. In the first step, we used the control inputs due to the actuator torques in order to control the body shape of the robot to a desired gait pattern. This induced a lateral undulatory motion on the robot. In the second step, we used the gait pattern parameters in the form of two compensators which controlled the orientation and planar position of the robot. Furthermore, we used the maneuvering controller to solve the formation control problem for a group of snake robots by synchronizing the commanded velocities of the robots. Generalization of the stability proofs to cluttered environments where the surface is not flat remains as a topic of future work. Also an extension of this work can be achieved by taking into account the possibility of collision between the robots during the convergence to their desired path.

## References

1. Hirose S (1993) "Biologically Inspired Robots: Snake-Like Locomotors and Manipulators." Oxford University Press.
2. Matsuno F, Sato H (2005) "Trajectory tracking control of snake robots based on dynamic model," in Proc. IEEE Int. Conf. on Robotics and Automation, pp. 3029-3034.
3. Date H, Hoshi Y, Sampei M (2000) "Locomotion control of a snake-like robot based on dynamic manipulability," in Proc. IEEE/RSJ Int. Conf. Intelligent Robots and Systems, Takamatsu, Japan.
4. Tanaka M, Matsuno F (2008) "Control of 3-dimensional snake robots by using redundancy." in Proc. IEEE Int. Conf. Robotics and Automation, pp. 1156-1161, USA.
5. Ma S, Ohmameuda Y, Inoue K, Li B (2003) "Control of a 3-dimensional snake-like robot." in Proc. IEEE Int. Conf. Rob. and Aut., (2):2067-2072, Taipei, Taiwan.
6. Tanaka M, Matsuno F (2006), "Cooperative Control of Two Snake Robots," Proc. IEEE Int. Conf. on Robotics and Automation, pp.400-405, Orlando, FL.
7. Tanaka M, Matsuno F, (2006) "Cooperative Control of Three Snake Robots," In Proc. of IEEE/RSJ Int. Conf. on Intelligent Robots and Systems, Florida, United States, pp. 3688-3693.
8. Prautsch P, Mita T, Iwasaki T (2000) "Analysis and control of a gait of snake robot." Trans. IEE J. Ind. Appl. Soc., 120-D:372381
9. McIsaac K, Ostrowski J (2003) "Motion planning for anguilliform locomotion." IEEE Trans. on Robotics and Automation, (19):637-652.
10. Hicks G, Ito K (2005) "A method for determination of optimal gaits with application to a snake-like serial-link structure." IEEE Trans. on Automatic Control, (50):1291-1306.
11. Ma S, Ohmameuda Y, Inoue K (2004) "Dynamic analysis of 3-dimensional snake robots," In Proc. IEEE/RSJ Int. Conf. Intelligent Robots and Systems, pp.767-772.
12. Ma S (2001) "Analysis of creeping locomotion of a snake-like robot," Advanced Robotics, 15(2):205-224.
13. Liljebäck P, Pettersen KY, Stavdahl Ø., Gravdahl JT (2013) "Snake Robots - Modelling, Mechatronics, and Control." Advances in Industrial Control, Springer.
14. Liljebäck P, Haugstuen IU, Pettersen KY (2012) "Path following control of planar snake robots using a cascaded approach," IEEE Trans. on Control Systems Technology, 20:111-126.
15. Rezapour E, Pettersen KY, Liljebäck P, Gravdahl JT, Kelasidi E (2014) "Path Following Control of Planar Snake Robots Using Virtual Holonomic Constraints: Theory and Experiments," Robotics and Biomimetics, Springer, 1:3.
16. Rezapour E, Pettersen KY, Gravdahl JT, Liljebäck P (2014) "Body Shape and Orientation Control for Locomotion of Biologically-Inspired Snake Robots," in Proc. 5th IEEE RAS/EMBS Int. Conf. on Biomedical Robotics and Biomechatronics, Sao Paulo, Brazil.
17. Mohammadi A, Rezapour E, Maggiore M, Pettersen KY (2014) "Direction Following Control of Planar Snake Robots Using Virtual Holonomic Constraints," in Proc. 53rd IEEE Conf. on Decision and Control (CDC 2014), Los Angeles, CA.
18. Rezapour E, Hofmann A, Pettersen KY, Mohammadi A, Maggiore M (2014) "Virtual Holonomic Constraints Based Direction Following Control of Snake Robots Described by a Simplified Model", in Proc. IEEE Multi-Conference on Systems and Control (MSC 2014), Antibes, France.
19. Rezapour E, Hofmann A, Pettersen KY (2014) "Maneuvering Control of Planar Snake Robots Based on a Simplified Model," in Proc. 2014 IEEE Int. Conf. on Robotics and Biomimetics, Bali, Indonesia.
20. Mohammadi A, Rezapour E, Maggiore M, Pettersen KY (2015) "Maneuvering Control of Planar Snake Robots Using Virtual Holonomic Constraints," IEEE Transactions on Control Systems Technology, DOI:10.1109/TCST.2015.2467208.
21. Liljebäck P, Pettersen KY, Stavdahl Ø, Gravdahl JT (2013) "Controllability and Stability Analysis of Planar Snake Robot Locomotion," IEEE Transactions on Automatic Control, 56(6):1365-1380.
22. Oh KK, Park MC, Ahn HS (2015), "A survey of multi-agent formation control," Automatica, vol. 53, pp.424-440.
23. Olfati-Saber (2006) "Flocking for multi-agent dynamic systems: algorithms and theory," IEEE Transactions on Automatic Control, 51(3):401-420.
24. Olfati-Saber R, Fax JA, Murray RM (2007) "Consensus and Cooperation in Networked Multi-Agent Systems," in Proc. of the IEEE, 95(1).215-233.
25. Mesbahi M, Egerstedt M (2010). Graph theoretic methods in multiagent networks. Princeton University Press.
26. Stilwell DJ, Bishop BE (2000) "Platoons of underwater vehicles," IEEE Control Systems Magazine, 20:45-52.
27. Scharf DP, Hadaegh FY, Ploen SR (2004) "A survey of space formation flying guidance and control (part 2)," in Proc. American Control Conf., Boston, Massachusetts.
28. Serrani A (2003) "Robust coordinated control of satellite formations subject to gravity perturbations," in Proc. of the American Control Conference, vol. 1, pp. 302307.
29. El-Hawwary MI, Maggiore M (2013) "Reduction theorems for stability of closed sets with application to backstepping control design," Automatica 49.1 pp. 214-222.
30. Westervelt ER, Grizzle JW, Chevallereau C, Choi JH, Morris B (2007) Feedback control of dynamic bipedal robot locomotion. Boca Raton: CRC press.
31. Maggiore M, Consolini L (2013) "Virtual Holonomic Constraints for Euler-Lagrange Systems," IEEE Trans. on Automatic Control, 58(4):1001-1008.
32. Shiriaev A, Perram JW, Canudas-de-Wit C (2005) "Constructive tool for orbital stabilization of underactuated nonlinear systems: Virtual constraints approach," IEEE Transactions on Automatic Control, 50.8:1164-1176.
33. Skjetne R (2005) "The maneuvering problem," NTNU, PhD-thesis.
34. Fossen TI (2002) "Marine control systems: Guidance, navigation and control of ships, rigs and underwater vehicles". Trondheim, Norway: Marine Cybernetics
35. Dacic DB, Nesic D, Teel AR, Wang W (2011) "Path following for nonlinear systems with unstable zero dynamics: an averaging solution". IEEE Transactions on Automatic Control. Vol. 56, pp.880-886.
36. Khalil H (2002) "Nonlinear Systems," Third edition, Prentice Hall.
37. Børhaug E, Pavlov A, Panteley E, Pettersen KY (2011) "Straight Line Path Following for Formations of Underactuated Marine Surface Vessels", IEEE Trans. on Control Systems Technology, Vol. 19, No. 3, pp. 493-506.
38. Børhaug E, Pavlov A, Pettersen KY (2006) "Cross-track formation control of underactuated surface vessels," In Proc. 45th IEEE Conference on Decision and Control, pp. 5955-5961.
39. Rezapour E (2015) "Model-based locomotion Control of Underactuated Snake Robots," PhD thesis, NTNU.